Aging and Stability of Microporous Sol-Gel-Modified Ceramic Membranes

Rob S. A. de Lange,† Klaas Keizer,* and Antonie J. Burggraaf

University of Twente, Faculty of Chemical Technology, Laboratory for Inorganic Chemistry, Materials Science and Catalysis, P.O. Box 217, 7500 AE Enschede, The Netherlands

Aging experiments on microporous sol-gel-derived nonsupported SiO_2 membranes were performed. Microstructure characterization was performed using nitrogen physisorption. It is found that both chemical aging and thermal aging result in densification of the microstructure, without pore growth. The influence of aging on supported SiO_2-modified membranes was investigated using gas permeation and separation experiments. As for the nonsupported materials, some densification takes place. This leads to lower permeation rates, but a strong positive effect was observed on the separation properties. This might be attributed to a decrease of the pore size. Separation factors ranging from 50 to 125 have been measured for H_2/CH_4 at temperatures in the order of 250 °C.

Introduction

Microporous [defined as $r_{pore} < 1$ nm (Sing, 1985)] SiO_2 membranes have gained increasing attention in the last few years because of interesting gas separation properties. Three main routes can be distinguished for the preparation of these membranes; these are modification of mesoporous [$1 < r_{pore} < 25$ nm (Sing, 1985)] ceramic membranes using sol-gel technology (Uhlhorn et al., 1992b; Kitao et al., 1990; de Lange et al., 1992; Brinker et al., 1993; Julbe et al., 1993), or by CVD (Okubo and Inoue, 1989; Gavalas et al., 1989; Tsapatsis et al., 1991; Kitao and Asaeda, 1991; Megiris and Glezer, 1992; Lin and Burggraaf, 1993), and leaching of hollow glass fibers (Bhandarkar et al., 1992; Shelekhin et al., 1992).

We have successfully obtained microporous SiO_2 membranes with molecular sievelike separation properties using sol-gel techniques (Uhlhorn et al., 1992b; de Lange et al., 1992, 1993, 1994, 1995a,b). Ultrathin (100 nm) silica and silica-based composite top layers have been prepared by a dip coating process of γ-alumina membranes with polymeric sols. The sols, prepared by acid-catalyzed hydrolysis and condensation of alkoxides, typically consist of polymeric inorganic structures with fractal dimensions in the order of 1.3 and radii of gyration of 20-30 Å (de Lange et al., 1994). The resulting membranes are microporous with very small pore sizes. For nonsupported membranes a pore-size distribution was calculated with a strong maximum at an effective pore diameter of 0.5 nm and a weak maximum is present at 0.75 nm (de Lange et al., 1993, 1994, 1995c).

These very small pores give rise to molecular sievelike gas transport properties, with typical activation energies for hydrogen permeation of 13 kJ mol^{-1} and permeation rates of 20×10^{-7} mol m^{-2} s^{-1} Pa^{-1} at 200 °C. Separation factors for H_2/CH_4 range from 40 up to 200 (de Lange et al., 1993, 1995b). From an extensive gas transport study (de Lange et al., 1993, 1995b), we concluded that the permeation mechanism can be seen as a series process involving internal sorption and micropore diffusion. Since at higher temperatures interface processes are not rate determining, the activation energy for permeation can be seen as an apparent activation energy, which includes the isosteric heat of adsorption (q^{st}) and the activation energy for micropore diffusion (E_1) by

$$E_{act} = E_1 - q^{st} \quad (1)$$

Mean values for the activation energies for micropore diffusion are 21 kJ mol^{-1} and 32 kJ mol^{-1} for H_2 and CO_2, respectively. Comparison with zeolite literature shows that these are relatively high values, in the order of values found for zeolite 4A (pore diameter 4 Å) or even higher. It was concluded that the pore size as calculated from nonsupported membranes is very likely an overestimate.

For practical applications of these membranes, not only the intrinsic gas separation properties are important, but also the stability of these membranes under process conditions. The thermal stability (where a low stability is defined by a strong tendency to crystallize in dry atmosphere) of silica is very high; crystallization hardly occurs below 900-1000 °C (Iler, 1979). The chemical stability, however, can be poor. For example, the presence of water at high temperatures may lead to breaking of Si-O-Si bonds at the surface, resulting in the formation of surface hydroxyl (Si-OH) groups (Scholze, 1982) and in densification and/or crystallization.

The surface chemistry of silica is an important parameter for the stability against water attack. The number and type of surface hydroxyl groups is strongly dependent on the temperature (van der Voort, 1990). At low temperatures ($T < 180$ °C) water is present on the surface, which is bonded to the surface hydroxyls with hydrogen bonds. Above 180 °C no "free water" is left, but only surface silanols, which are bridged with neighboring hydroxyls by hydrogen bonds at high coverages. At higher temperatures ($T > 300$ °C), dehydroxylation takes place and isolated hydroxyls are present. Dehydroxylation by thermal treatment can reduce the number of surface hydroxyls from 4-6 per square nanometer at 200 °C to 1-2 per square nanometer at 800 °C at free surfaces. Full thermal dehydroxylation, which is a reversible process, thus needs very high temperatures. The surface is then less sensitive for attack by water since it is now hydrophobic.

* Author to whom correspondence should be addressed.

† Present address: Flexovit Produktie b.v., Research & Development, P.O. Box 10, 7150 AA Eibergen, The Netherlands.

0888-5885/95/2634-3838$09.00/0

However, hydroxyls are more strongly bonded in pores due to the surface curvature. For example, at 600 °C the number of hydroxyls per square nanometer is 6 for pores with diameters of 10 Å, while for wider pores of respectively 20 and 27 Å only 4.8 and 3.6 hydroxyl groups are present per square nanometer (Brinker and Scherer, 1992, Chapter 10).

As shown by Nam and Gavalas (Gavalas et al., 1989; Nam and Gavalas, 1989), aging (high temperature with water) of SiO_2 membranes, which were derived by CVD modification, results in a decreased hydrogen permeation and increased nitrogen permeation. This opposite effect was explained by densification of the layer. The hydrogen permeation, which is initially 2 orders of magnitude higher than the nitrogen permeation, takes place mainly through the SiO_2 top layer. This top layer, however, is impermeable for nitrogen. Consequently, nitrogen can only permeate through defects. Due to aging, resulting in densification of the top layer, the hydrogen permeation decreases, but since microcracks may be formed, the nitrogen permeation can increase.

In this paper, the results of a stability study of microporous silica membranes are discussed. These experiments are performed both on nonsupported and supported membranes, and include pore size characterization and determination of the transport properties. Characterization of nonsupported membrane top layers is inevitable unfortunately, because with the present state of technology one is still unable to characterize the pore size of the supported ultrathin microporous material. As has been reported in earlier work (de Lange et al., 1993, 1995a–c), comparison of the microstructure of supported and nonsupported microporous membranes is difficult, but can be performed with care.

For the present system, it is found that nonsupported membranes will very probably have a slightly larger pore size (pore diameter in the order of 0.5 nm) than supported ones (pore diameter in the order of < 0.4 nm). As discussed before extensively, this difference is caused by the difference in drying rate of the formed wet gel (de Lange et al., 1995c). We think this difference is small enough for the quantitative aging studies as presented, and the results in structural evolution of nonsupported membranes are indicative for the supported ones.

The influence of aging on pore size and porosity, and consequently on gas transport properties, is very important from a technological point of view because strong changes in membrane performance in practical application cannot be tolerated.

Experimental Section

Membrane Formation. γ-Alumina membranes were prepared by a dip coating process of α-alumina supports (disk shape, diameter 39 mm, thickness 2 mm, mean pore radius 160 nm, porosity 50%) in boehmite (γ-AlOOH) dip solutions (Uhlhorn et al., 1992a). The membranes were dried in a climate chamber for 3 h (40 °C, 60% relative humidity) prior to calcination in static air for 3 h at 600 °C (heating and cooling rate 60 °C per hour). Depending on membrane quality, this procedure is repeated one or two times to obtain a defect-free membrane; the final top layer thickness is in the order of 7–10 μm, with a mean pore diameter of around 5 nm.

Polymeric silica sols were prepared using TEOS (tetraethyl orthosilicate, Merck, p.a.), ethanol (Merck, p.a.), HNO_3 (Merck, p.a.), and demineralized water. A mixture of acid and water was carefully added to the TEOS/ethanol solution using a dropping funnel. The reaction mixture was refluxed for 3 h at 80 °C under stirring. The standard sol composition ($StSiO_2$) is given by the molar ratios: $TEOS/H_2O/ethanol/HNO_3 = 1/6.4/3.8/0.085$.

Nonsupported microporous membranes were prepared by drying the sols in petri dishes. Drying took place overnight under ambient conditions (identical standard samples, codes beginning with A..) or over 3 h in a climate chamber (identical standard samples, codes beginning with C..) at 40 °C and 60% relative humidity and turbulent aerodynamic conditions (Hereaus Vötsch VTRK 300, wind velocity 3.25 m s^{-1}). The resulting material consists of flakes on the order of 2 mm.

Supported microporous membranes (thickness 100 nm) were prepared by modification of γ-alumina membranes with diluted (18 times with ethanol) SiO_2 sols using a dip coating process. Membranes were dipped for 4 s (pull-out rate 2 cm s^{-1}) and allowed to dry at ambient for about 30 s. A more detailed description of the sol synthesis and membrane formation is given elsewhere (de Lange et al., 1993, 1994, 1995a).

Membrane codes are given as Alx–Siy–z, where x corresponds to the number of γ-alumina dipping steps, y corresponds to the number of silica modification steps, and z corresponds to the specific membrane in question.

The dried supported and nonsupported membranes were calcined in static air at 400 °C for 3 h, with a heating and cooling rate of 25 °C per hour.

Nitrogen Physisorption. Nitrogen adsorption measurements were performed with a Carlo Erba Sorptomatic 1900, extended with a turbo molecular pump system (Leybold PT50) and an extra pressure transducer (MKS Baratron type 122A) for the low-pressure range (10^{-3} Torr to 10 Torr, accuracy 0.5% of reading, lowest suggested pressure reading 3×10^{-3} Torr). All samples were degassed for 23 h at 350 °C at 10^{-6} Torr. The experimental error in the total adsorbed volume, mainly caused by weighing errors, has found to be in the order of 5%.

The method developed by Horváth and Kawazoe (Horváth and Kawazoe, 1983) for pore-size assessment in microporous, slit-shaped carbon using CO_2, and modified by Saito and Foley (Saito and Foley, 1991) for cylindrical pore geometry was selected for the pore size analysis of the nonsupported membranes. We have further modified this method for N_2 adsorption on silica (de Lange et al., 1993, 1995c). The t-plot method (Lippens and de Boer, 1965) and the Dubinin–Radushkevich (DR) method (Dubinin, 1960; eq 2), are used for the determination of the micropore volume:

$$V = V_0 e^{-(A/E)^2} \tag{2}$$

V is the amount adsorbed at relative pressure P/P_0 and V_0 is the micropore volume, $A = RT \ln(P_0/P)$ is the adsorption potential (J mol^{-1}), where R is the gas constant (J mol^{-1} K^{-1}) and T is the temperature (K), and E is an energy constant (J mol^{-1}). [E is used in some limited cases for pore size assessment (Dubinin, 1960; de Lange et al., 1993, 1995c; Sing et al, 1985).]

The micropore volume is calculated directly from the isotherm, from the intercept of the straight line through the plateau with the adsorption axis. We will refer to this as the "intercept method". This is a more accurate estimate of the micropore volume than by taking the volume adsorbed at $P/P_0 = 0.95$, which is often used in literature, since it excludes the contribution of the

external surface. The determination of the micropore volume according to the t-plot method is not always very straightforward. In these cases a minimum and maximum micropore volume will be given. The pore volume is calculated from the amount gas adsorbed by V_{pore} (mL g^{-1}) = V_{ads} (mL(STP) g^{-1}) × (1.547×10^{-3}) (Gregg and Sing, 1982). The density of adsorbed nitrogen in the micropores was estimated by taking the density of liquid nitrogen (0.808 g mL^{-1}). Porosities are calculated by

$$\epsilon\,(\%) = \frac{V_p}{V_p + (1/\rho)} \times 100 \qquad (3)$$

where V_p is the pore volume (mL g^{-1}), and ρ is the density of the solid phase (g mL^{-1}).

Gas Permeation and Separation. Gas permeation experiments were performed by measurement of dead-end permeation. The disk-shaped membranes were placed in stainless steel cells (F. M. Velterop b.v., Enschede, The Netherlands, cell R 250), with the top layer at the feed side. Kalrez (DuPont) sealings were used, with a measuring area of 1.911 cm^2, and maximum process temperature 300 °C. The low pressure side of was evacuated (P < 0.01 bar). The permeation is expressed in mol m^{-2} s^{-1} Pa^{-1} (≡1.344×10^7 mL min^{-1} cm^{-2} bar^{-1} ≡ 1.93×10^8 m^3 m^{-2} day^{-1} bar^{-1}). The used gases were > 99.9% pure (propene, *n*-butane, and isobutane 99.5%).

For the calculation of the true microporous top layer performance, the permeation results have to be corrected for the pressure drop over the γ-alumina membrane. This correction procedure (de Lange et al., 1993, 1995a,b) involves the calculation of the pressure at the interface of top layer and the γ-alumina membrane. This allows the calculation of the actual top layer permeation, which is the ratio of the flux (mol m^{-2} s^{-1}) and the pressure drop over the top layer ($P_{high}-P_{interface}$).

Gas separation experiments were performed using binary gas mixtures in equipment as described extensively elsewhere (de Lange et al., 1993, 1995a,b). Experiments were mainly performed in the countercurrent mode, in stainless steel membrane test cells (F. M. Velterop b.v., cell R 250), with Kalrez sealing rings (DuPont) and a measuring area of 1.911 cm^{-2}. The binary gas mixture was led along the microporous top layer at the high-pressure side. Argon was used as sweep gas at the permeate side, which was connected to a vacuum pump.

The separation factor (α), defined as the enrichment factor of one component in the permeate compared to feed composition, is given by

$$\alpha = \frac{y}{1-y}\frac{1-x}{x} \qquad (4)$$

where y is the molar fraction of the faster permeating component in the permeate and x is the molar fraction of this component in the feed.

Microporous membranes were degassed prior to the permeation and separation measurements, in order to remove adsorbed water from the micropores, by overnight heating to 200 °C with a hydrogen flow of 1 mL min^{-1} and the low pressure side connected to the vacuum pump.

Aging Experiments. Low-temperature aging experiments were performed among others by placing supported as well as nonsupported membranes in the climate chamber (40 °C/60% relative humidity). These conditions are chosen to investigate the ambient stability of membranes, which is among others relevant for handling under normal (laboratory) atmospheric conditions.

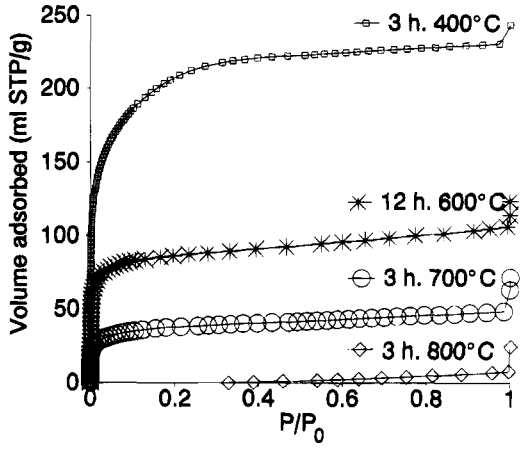

Figure 1. N_2 adsorption isotherms of microporous sol–gel-derived silica sample AH calcined at different temperatures.

High-temperature aging experiments were performed by placing the nonsupported (350 °C) and supported membranes (250 °C, membrane in test cell) in a furnace, and flushing argon (10 mL min^{-1}) at atmospheric pressure over the membrane material. To study the influence of water, the argon stream was led through water at 15 °C, leading to a relative water vapor pressure of 1.7% at atmospheric pressure. These conditions are chosen to get near industrial conditions for e.g. dehydrogenation processes, where a few percent of water may be present at temperatures of 400–600 °C [the maximum temperature for our experiments (250 °C for supported membranes) is determined by the test cells].

Results

Stability of Nonsupported Microporous SiO_2. In Figure 1, the N_2-adsorption isotherms are shown for a nonsupported silica sample AH, prepared from a standard SiO_2 sol (dried overnight at ambient conditions) with different calcination treatments to investigate the structural evolution of the sol–gel-derived silica dried gel. As can be seen clearly, increase of calcination temperature, compared to the standard treatment (3 h, 400 °C), results in a strong decrease of the pore volume. However, the shape of the isotherms remains type I (except for 3 h at 800 °C), which is indicative for microporous materials (Sing et al., 1985).

The corresponding pore size distributions (PSD's), according to the modified Horváth-Kawazoe (HK) model are given in Figure 2. The pore size distribution for as-prepared silica calcined at 400 °C shows a strong maximum at an effective pore diameter of 0.5 nm, and a weaker maximum at around 0.75 nm, which is typical for these samples as shown previously (de Lange et al., 1993, 1994, 1995c). As can be seen, the pore volume is decreased and the distribution is slightly shifted to lower pore diameters for the samples calcined at higher temperatures. The calculated micropore volumes and porosities have been summarized in Table 1. In this table, also an experiment is reported where a calcined sample (sample CC, prepared from a standard SiO_2 sol, dried for 3 h in the climate chamber) is exposed to a second calcination procedure. Between the two calcination procedures the sample was exposed to ambient air for 1 day. The second calcination procedure consists of

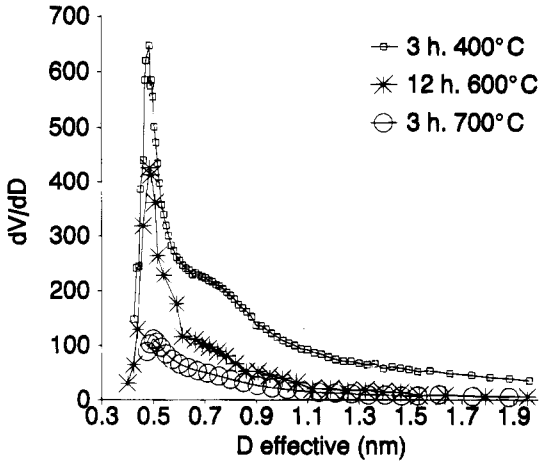

Figure 2. Horváth–Kawazoe pore size distribution of microporous sol–gel-derived silica sample AH calcined at different temperatures.

Table 1. Thermal Stability of Nonsupported Silica Membranes: Micropore Volumes Using the *t*-Plot, the Dubinin–Radushkevich Method and the "Isotherm Intercept" Method; Porosities Calculated with the "Isotherm Intercept" Method

	V_{micro} (cm^3 g^{-1})			
sample	*t*-plot[b]	DR	isotherm intercept	porosity[a] (%)
AH, 3 h, 400 °C	0.324/0.351	0.266	0.331	42
AH, 12 h, 600 °C	0.116/0.147	0.13	0.124	21
AH, 3 h, 700 °C	0.046/0.070	0.056	0.054	11
AH, 3 h, 800 °C	–	–	–	0
CC, 3 h, 400 °C	0.176/0.189	0.184	0.175	28
CC, 3 h, 400 °C + 3 h, 400 °C/ 3 h, 600 °C	–	–	–	0

[a] Calculated on the basis of a skeletal density of amorphous silica of 2.2 g cm^{-3}. [b] Calculated from a fit in the region $3 < t < 9$ (first figure) and from a fit of the plateau region.

a first treatment for 3 h at 400 °C and a second treatment for 3 h at 600 °C (heating and cooling rates 25 °C per hour). The finally obtained material was now completely dense for nitrogen adsorption.

Low temperature chemical stability was investigated among others by ambient aging of microporous silica sample AE (prepared from a standard sol, dried overnight under ambient conditions, and calcined at 400 °C for 3 h). The pore size distributions are shown in Figure 3. The micropore volume, and consequently the porosity, of the material decrease during aging, as reported in Table 2. The porosity is decreased from 38% to 31% after 16 months. The shape of the pore size distribution is not affected by the aging treatment, but only a small subtle shift to smaller pore diameter is present.

Pore-size distributions obtained from low-temperature aging experiments of sample AH (40 °C, 60% relative humidity) are shown in Figure 4. The volume adsorbed decreases continuously as function of aging time, and the porosity decreases from 42% for the as-prepared sample to 31% after 80 days of aging (Table 2). The shape of the pore size distribution, given in Figure 4, does not change.

High-temperature aging of silica samples CC and CD (both prepared from standard silica sols, dried for 3 h in the climate chamber, and calcined at 400 °C for 3 h) resulted only in a very minor decrease of the pore volumes and porosities, as can be seen from Figure 5

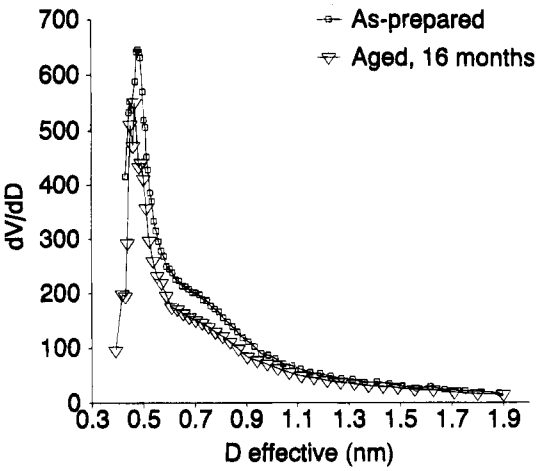

Figure 3. Horváth–Kawazoe pore size distribution of as-prepared silica (sample AE) and aged for 16 months at ambient conditions.

Table 2. Chemical Stability of Nonsupported Silica Membranes: Micropore Volumes Using the *t*-Plot, the Dubinin–Radushkevich Method, and the "Isotherm Intercept" Method; Porosities Calculated with the "Isotherm Intercept" Method

	V_{micro} (cm^3 g^{-1})			
sample	*t*-plot[b]	DR	isotherm intercept	porosity[a] (%)
AH	0.324/0.351	0.266	0.331	42
AH, 22 days[c]	0.302/0.317	0.250	0.305	40
AH, 51 days[c]	0.251/0.282	0.213	0.257	36
AH, 80 days[c]	0.217/0.248	0.172	0.215	31
AE	0.260/0.285	0.261	0.277	38
AE, 16 months[d]	0.213/0.229	0.194	0.206	31
CC	0.176/0.189	0.184	0.175	28
CC, 10 days[e]	0.142/0.170	0.160	0.152	25
CD	0.170/0.172	0.177	0.170	27
CD, 10 days[f]	0.147/0.162	0.164	0.152	25

[a] Calculated on the basis of a skeletal density of amorphous silica of 2.2 g cm^{-3}. [b] Calculated from a fit in the region $3 < t < 9$ (first figure) and from a fit of the plateau region. [c] 40 °C, 60% relative humidity. [d] Ambient. [e] 350 °C under Ar. [f] 350 °C under Ar + H_2O (1.7%).

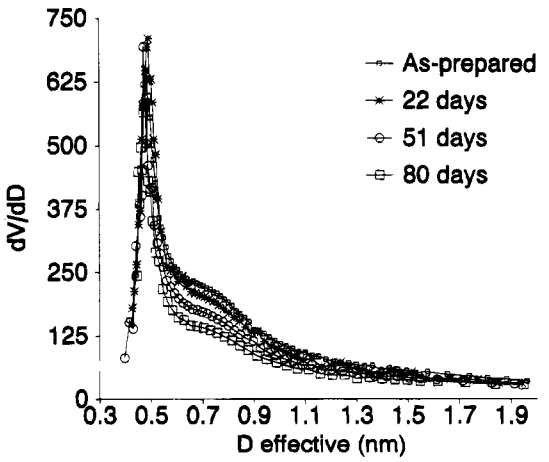

Figure 4. Horváth–Kawazoe pore size distribution of as-prepared silica AH and after aging (40 °C, 60% relative humidity).

and Table 2. The presence of water (1.7%) does not show to result in an increased aging at this temperature, as can be seen by comparison of the decrease of porosity of sample CC and CD (aged in the presence of water). The calculated PSD's (Figure 6) are identical for the as-prepared samples and the aged samples.

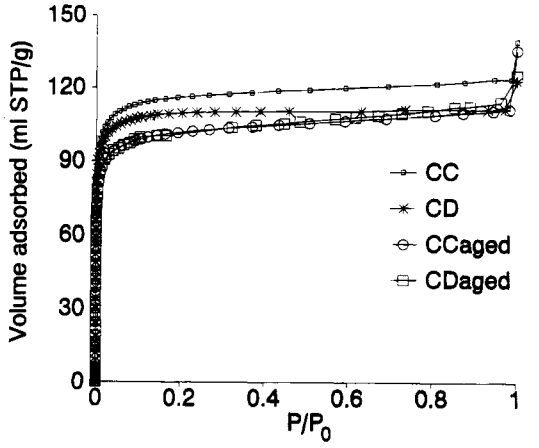

Figure 5. N_2 adsorption isotherms of as-prepared silica CC and CD and aged for 10 days at 350 °C under argon, sample CD with 1.7% H_2O.

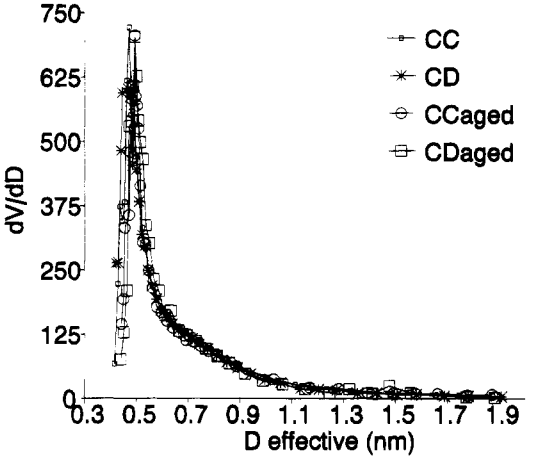

Figure 6. HK pore size distribution of as-prepared silica CC and CD and aged for 10 days at 350 °C under argon, sample CD with 1.7% H_2O.

Stability of Supported Microporous Membranes. Results from aging experiments on supported silica modified membranes are presented in this section. Firstly, low-temperature chemical aging will be discussed. These experiments were performed by exposing the membranes to water-containing atmospheres. Secondly, thermal aging, in the absence of water, will be discussed. Since calcination of dried silica modified membranes at 600 °C can also be considered as a thermal aging procedure (calcination at 400 °C is the standard procedure), these experiments are included as well. Thirdly, results of chemical aging experiments at high temperatures are presented. The effect of aging is discussed, and finally some additional separation properties of the aged membranes are presented.

Low-Temperature Chemical Aging. In Table 3, the results are given for an aging experiment (10 days at 40 °C/60% relative humidity) with supported silica modified membrane Al1−Si1−C. The γ-alumina membrane was prepared by a single standard coating (dipping/drying and calcination) procedure, and silica was modified in a single step using the standard conditions. The membrane was characterized by hydrogen permeation measurements before the aging treatment. The permeation rates, noncorrected as well as corrected for support influence, and (apparent) activation energies for hydrogen permeation are given. Then it was aged, with the membrane in the permeation cell, in the climate chamber. After the aging treatment hydrogen permeation was measured again to investigate the effect of the aging procedure. CO_2 and CH_4 permeation for the aged membrane were measured as well. Two main effects can be seen from this experiment. Firstly, the hydrogen permeation rates are decreased after the aging treatment. This effect is strong for the corrected permeation rates, where a decrease from 61×10^{-7} mol m^{-2} s^{-1} Pa^{-1} to 15.3×10^{-7} mol.m^{-2}.s^{-1}.Pa^{-1} at 250 °C is calculated. Secondly, the dependency of the hydrogen permeation of temperature is less strong after aging. This results in a decrease of the activation energies for hydrogen permeation from 11.0 kJ mol^{-1} to 6.2 kJ mol^{-1}.

Table 3. Permeation Characteristics of Silica-Modified Membrane Al1−Si1−C, as Prepared, and after 10 days Aging at 40 °C/60% Relative Humidity[a]

	as-prepared ↓	aged ↓ →		
T (°C)	F^b (H_2)	F^b (H_2)	F^b (CO_2)	F^b (CH_4)
50	9 *11*	5.9 *6.9*	3.0	2.66
100	16.5 *30*	6.5 *8.1*		
150	20.3 *44*	7.9 *10.0*	2.9	2.24
200	21.5 *55*	8.2 *10.9*		
250	21.9 *61*	10.5 *15.3*	2.5	2.0
E_{act} → (kJ mol^{-1})	6.5 *11.0*	3.8 *6.2*		

[a] P_{low} = 0 bar; P_{high} = 1 bar. [b] Permeation in (10^{-7} mol m^{-2} s^{-1} Pa^{-1}); italic values are corrected for support influence.

From the results obtained with the nonsupported membranes, it is known that aging leads to densification of the materials. This can explain the lower permeation rate for hydrogen after aging. Obviously, some cracking occurred, since the activation energy for hydrogen permeation is decreased. If cracking occurs due to increased densification during aging, the permeation will of course increase with respect to the situation just before cracking. However, with respect to the nonaged membrane, the permeation can be lower due to the densification process.

As can be seen, the carbon dioxide permeation and the methane permeation decrease as function of temperature and are at 200 °C a factor 4−5 lower than the hydrogen permeation rate.

It has to be noted that the result of aging looks to be more severe for this supported membrane than for nonsupported silica membranes aged under this condition. As can be seen from Table 2, the porosity of the nonsupported membranes is only decreased from 42% to 40% after 22 days aging at these conditions. This point will be discussed further.

Silica-modified membrane Al3−Si1−M, prepared by a single modification step with silica of a γ-alumina membrane which was prepared by three boehmite dipping steps, was aged (40 °C/60% relative humidity for 17 days) directly after the silica calcination step. The separation properties for H_2/CH_4 after this aging procedure are shown in Figure 7. As can be seen very high H_2/CH_4 separation factors were obtained. Separation measurements were performed the next few days, after cooling down the membrane. The system showed a little higher separation factor of 108 at 100 °C, which proved to be stable up to 5 days.

Mean H_2/CH_4 separation factor values for the freshly prepared membranes are in the order of around 30−40 at 100 °C, with a single extreme of around 200 (de Lange et al., 1993, 1995b). The H_2/CH_4 separation factor found for this membrane is therefore significantly higher. This result suggests that aging does not necessarily lead to decreased gas separation properties in every case.

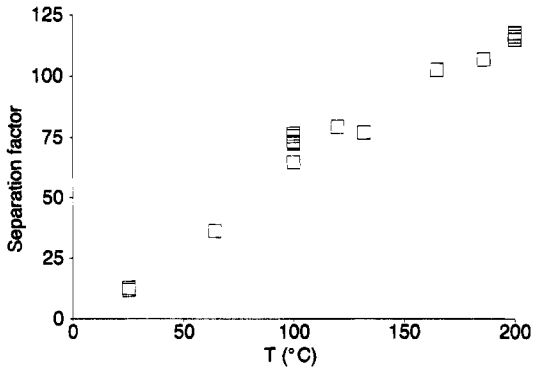

Figure 7. H_2/CH_4 separation of membrane Al3−Si1−M, after aging for 17 days at 40 °C and 60% relative humidity Feed 100/100 mL min^{-1}, Ar sweep gas 200 mL min^{-1}, ΔP = 1.8 bar; P_{low} = 0.7 bar.

Table 4. H_2 and CH_4 Dead End Permeation for Aged (200 °C, 4 months, Dry) Silica-Modified Membranes Al3−Si1−O and Al3−Si1−P

membrane	treatment	P_{feed}[a] (bar)	F^b (H_2)	F^b (CH_4)	perm-selectivity
Al3−Si1−O	as-prepared	1.8	8.9	0.4	22.4
Al3−Si1−O	aged	3.0	6.8	0.26	26.3
Al3−Si1−P	as-prepared	1.7	4.0	0.09	42.2
Al3−Si1−P	aged	2.9	2.7	0.08	31.4

[a] Composition 50/50 H_2/CH_4. [b] 10^{-7} mol m^{-2} s^{-1} Pa^{-1}, at 20 °C.

High-Temperature Thermal Aging. Membranes Al3−Si1−O and Al3−Si1−P, both prepared by a single modification of a γ-alumina membrane prepared by three boehmite dipping steps, are exposed to 200 °C (dry atmosphere) for 4 months. The effect of this treatment was investigated by permeation experiments using binary gas mixtures. The results are given in Table 4.

Aging for 4 months at 200 °C resulted in a decrease of the permeation rate of 24% for Al3−Si1−O and 33% for Al3−Si1−P, while the permselectivity increased for Al3−Si1−O from 22.4 to 26.3, but decreased from 42.2 to 31.4 for Al3−Si1−P. This observation supports the impression from the other experiments that aging leads to densification, but does not necessarily lead to cracking (giving lower separation factors) in all cases (e.g. Al3−Si1−M).

The synthesis of SiO_2-modified membranes prepared at an increased calcination temperature of 600 °C, which is in fact a thermal aging treatment, with high-quality top layers proved to be difficult. To judge the membrane quality, the activation energy for hydrogen permeation can be used (de Lange et al., 1993, 1995b). High-quality SiO_2-modified membranes have typical hydrogen activation energies higher than around 7−8 kJ mol^{-1} (corrected for support influence). Calcination in a single step at 600 °C (for 3 h and 25 °C per hour heating and cooling rate) directly after membrane formation, or in a two-step calcination procedure (3 h at 400 °C, followed by 2 h at 600 °C), was not successful. The best results were obtained by a two-step silica modification, with a two-step calcination procedure. Membranes Al3−Si2−600A and Al3−Si2−600B were obtained by modification of γ-alumina membranes, which were prepared by a three-step dipping procedure with boehmite. The first silica modification step was performed with standard silica dip solutions. This was followed by calcination for 3 h at 400 °C, directly followed by 3 h calcination at 600 °C; heating and cooling rates are 25 °C per hour. Subsequently, the membranes were modified in a second step with 10 times more diluted silica dip solutions, followed by the same calcination procedure. The results have been summarized in Table 5. Both membranes showed only very slightly activated transport for hydrogen, with activation energies, after support correction, of only 4.8 kJ mol^{-1} and 5.0 kJ mol^{-1}. The CH_4 permeation for membrane Al3−Si2−600B is activated too, with an activation energy of 5 kJ mol^{-1} after support correction; both the CO_2 and O_2 permeation are not activated. The permselectivity for H_2/CH_4 at 250 °C is around 20.

Table 5. Permeation Results for Two-Step Silica-Modified Membranes Al3−Si2−600A and Al3−Si2−600B, Calcined at 600 °C

	Al3−Si2−600A ↓	Al3−Si2−600B ↓ →			
T (°C)	F^a (H_2)	F^a (H_2)	F^a (CH_4)	F^a (CO_2)	F^b (O_2)
50	6.5 *8.0*	13.8 *23*	1.1 *1.23*	5.0	
100	8.7 *12.3*				4.7
150	9.4 *13.9*	16.0 *35*	1.4 *1.65*	4.0	4.0
200	10.3 *16.6*				
250	10.3 *17.0*	17.0 *48*	1.9 *2.45*	3.2	3.7
E_{act} → (kJ mol^{-1})	3.1 *4.8*	1.6 *5.1*	3.8 *5.0*		

[a] Permeation in 10^{-7} mol m^{-2} s^{-1} Pa^{-1}; italic values corrected for support influence.

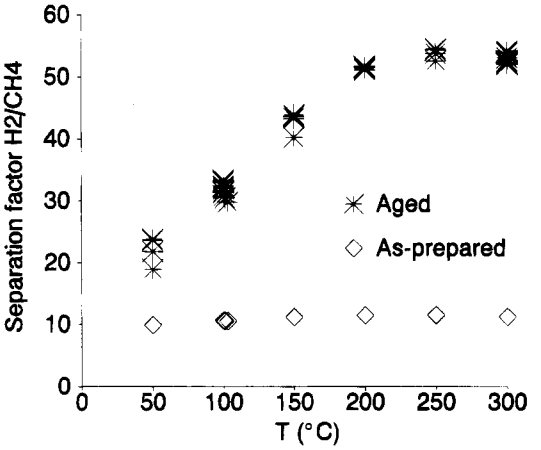

Figure 8. H_2/CH_4 separation of membrane All−Si2−A before and after aging (10 days 250 °C, Ar + 1.7% H_2O). Feed: 200/200 mL min^{-1} H_2/CH_4. ΔP = 0.4 bar; P_{low} = 0.7 bar.

High-Temperature Chemical Aging. High-temperature aging [250 °C for 10 days under argon and water (1.7%)] was investigated with silica-modified membrane All−Si2−A, prepared by two-step modification with polymeric silica of a γ-alumina membrane, which was prepared in a single boehmite dipping procedure. For both modification steps a standard calcination procedure was followed (3 h, 400 °C). During the aging treatment, the membrane was kept in the membrane cell to avoid possible damage due to membrane handling. To study the effect of aging, the H_2/CH_4 separation and H_2/isobutane separation are compared before and after the aging treatment. This is shown in Figures 8 and 9, respectively.

The gas separation properties before the aging treatment have been extensively discussed elsewhere (de Lange et al., 1993, 1995b). The H_2/CH_4 separation factor of the nonaged membrane slightly increases as function of temperature to a maximum of 11 at 200−

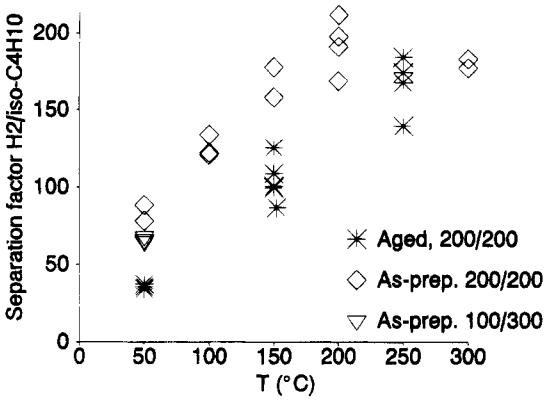

Figure 9. H_2/isobutane separation of membrane All−Si2−A before and after aging (10 days 250 °C, Ar + 1.7% H_2O). Feed in mL min^{-1} for H_2/isobutane. ΔP = 0.7 bar; P_{low} = 0.7 bar.

Table 6. H_2/CH_4 Separation and H_2 Permeation of Silica-Modified Membrane All−Si2−A as Function of Treatment

	F^a (H_2)		α (250 °C)	
	50 °C	200 °C	H_2/CH_4	H_2/iso-C_4H_{10}
as-prepared	18.6	24.6	6	160
second dipping	10.4	14.1	11	180
aging	6.0	9.7	55	160

[a] Permeation in 10^{-7} mol m^{-2} s^{-1} Pa^{-1}.

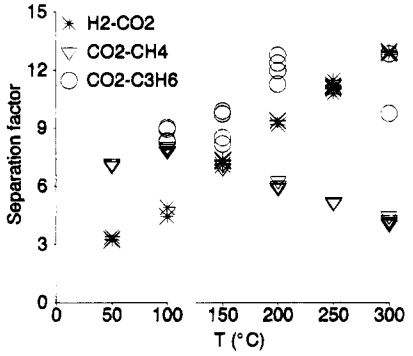

Figure 10. CO_2/−separation of membrane All−Si2−A after aging (10 days 250 °C, Ar + 1.7% H_2O). Feed compositions and pressures given in Table 8.

300 °C; the H_2/isobutane separation factor is considerably higher, with a maximum of around 200 at 200 °C. Aging results in considerably improved H_2/CH_4 separation factors, with a maximum around 55 at 250 °C. The H_2/isobutane separation, however, decreases slightly.

In Table 6, the hydrogen permeation rates and separation factors are given for this membrane after the first and second silica modification, and after the aging treatment. The improvement of the H_2/CH_4 separation factor is accompanied by a decrease in permeation rate, which is roughly a factor 3 when the multiple-dipped, and aged membrane is compared with the as-prepared membrane.

Some Gas Separation Properties of Aged Membrane All−Si2−A. Separation experiments with aged membrane All−Si2−A involving CO_2 are given in Figure 10. The H_2/CO_2 separation factor increases continuously as function of temperature to a maximum of 13 at 300 °C. The CO_2/C_3H_6 separation factor increases less strong with temperature, the maximum is of the same order, about 12 at 200−300 °C. A distinct optimum, however, in separation factor as function of

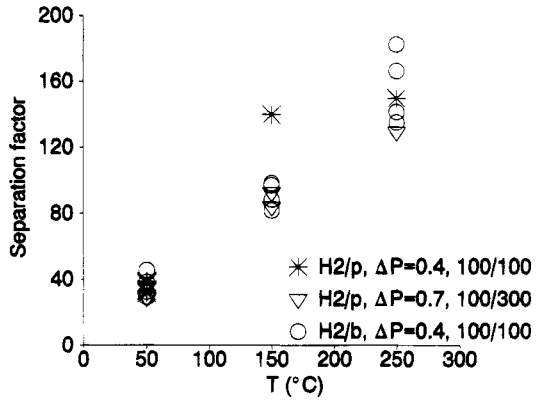

Figure 11. H_2/propene (p) and H_2/*n*-butane (b) separation of membrane All−Si2−A after aging (10 days 250 °C, Ar + 1.7% H_2O). Feed in mL min^{-1} H_2/−, P_{low} = 0.7 bar.

Table 7. Summary of Separation Results of Aged Silica Membrane All−Si2−A[a]

system	α (250 °C)	ΔP (bar)	feed (mL min^{-1})
H_2/CO_2	11	0.7	200/200
H_2/CH_4	60	0.4	100/100
H_2/CH_4	60	0.4	175/25
H_2/CH_4	60	1.3	175/25
H_2/propene	140	0.4	100/100
	130	0.8	100/300
H_2/butane	160	0.4	100/100
H_2/isobutane	160	0.7	200/200
CO_2/CH_4	5	0.5	100/100
CO_2/propene	10	1.7	100/200

[a] Note: $P_{low} \approx$ 0.7 bar; Ar sweep gas flow = 150 mL min^{-1}.

Table 8. Effect of Feed Pressure and Composition on Separation Factor for Aged Silica-Modified Membrane All−Si2−A[a]

system	feed (mL min^{-1}) H_2/−	ΔP (bar)	α (50 °C)
H_2/propene[b]	100/100	0.4	35
	200/200	0.7	30
	200/200	1.7	16
	100/300	0.7	29
H_2/isobutane[c]	200/200	0.7	83
	100/300	1.9	68

[a] Note: $P_{low} \approx$ 0.7 bar; Ar sweep gas flow = 150 mL min^{-1}. [b] Obtained after the aging experiment. [c] Obtained after the second modification step.

temperature can be seen for CO_2/CH_4 (where CO_2 is the fastest permeating component).

The H_2/propene and H_2/*n*-butane separation factors, as given in Figure 11, are comparable, with maxima of around 160 for H_2/*n*-butane and 140 for H_2/propene at 250 °C. A summary of some separation data has been given in Table 7. It can be clearly seen that the separation factors for binary gas mixtures with H_2 increase with the size of the second gas molecule (CO_2 < CH_4 < C_3H_6 < *i*-C_4H_{10}). This has been observed for freshly prepared membranes as well.

In Table 8, the influence of process parameters like feed composition and feed pressure is shown for two limited experiments. For H_2/propene it can be seen that the influence of an increased feed pressure from 0.4 to 0.7, which is obtained by an increased feed flow, results in a decrease of the separation factor from 35 to 30. A further increase of the pressure, with the same feed flow, results in a decrease of the separation factor to 16. Changing the feed composition from 200/200 to 100/300 (H_2/propene in milliliters per minute), with a constant pressure (ΔP = 0.7 bar) and total feed flow (400

mL min^{-1}), does not result in a significant decrease of the separation factor (decrease from 30 to 29).

For H_2/isobutane it is also observed that an increased pressure results in a decreased separation factor from 83 to 68. The influence of the different feed composition is of less importance, as has been shown for H_2/propene.

Discussion

Stability of Nonsupported Membranes. The porosity of silica calcined for 3 h at 400 °C, which is the standard procedure, is typically in the order of 35–40%. The pore size calculation from the N_2 adsorption isotherms gives a pore size distribution with a strong maximum at an effective pore diameter of 0.5 nm and a weaker maximum at around 0.75 nm. Both thermal aging and chemical aging, however, lead to a decrease in pore volume, and consequently, the porosity of microporous sol–gel-derived silica.

Thermal aging by calcination at 600 °C for 12 h, and 3 h at 700 °C, for example, lead to a decrease in porosity to 21% and 11%, respectively. Calcination at 800 °C as well as a two-step calcination procedure of an aged sample to a maximum of 600 °C (Table 1) lead to complete densification of silica.

The chemical stability is rather good at temperatures < 350 °C. After 80 days at 40 °C and 60% relative humidity the porosity is decreased from 42% to 31%. Aging for 10 days at 350 °C with 1.7% H_2O, resulted in a very small decrease of porosity from 27% to 25%.

It is quite remarkable that both thermal and chemical aging treatments do not lead to pore growth of the microporous materials. The PSD's remain of roughly the same shape, and even a decrease in pore size seems to occur. This can be seen by a slight decrease of the relative contribution of the peak at 0.75 nm. It has to be recognized, however, that the minimum pore size which can be detected is around 0.4 nm, as we have shown before (de Lange, 1993, 1995c). If indeed the pore size is gradually decreased for the whole PSD, then also pores will be formed below this detection limit. Consequently, the porosity calculated by N_2 adsorption may be too low.

On a microscopic scale, aging seems to result in comparable structural evolution as observed for viscous sintering at higher temperatures for sol–gel-derived silica (Brinker and Scherer, 1992; Chapter 9). Viscous sintering leads to a decrease of porosity and a gradual decrease of pore size. One of the processes which takes place is internal condensation of the hydroxyl groups in the pores. It is remarkable that even at low temperatures relatively strong effects have been found. However, the samples have to be degassed thoroughly prior to the adsorption measurements in order to remove adsorbed gases and water (at 350 °C for 24 h). This treatment may also cause additional densification since water is adsorbed in the pores, giving rise to further condensation reactions of the surface hydroxyls. The presence of water is obviously important for this, since it is known that a second degassing process for samples which were not exposed to the atmosphere did not influence the measured porosity.

The addition of TiO_2, ZrO_2, or Al_2O_3 was expected to improve the stability of microporous SiO_2. We have successfully obtained 100% microporous materials with up to 30 mol % MO_x (x = Ti, Al, Zr) (de Lange, 1993, 1994, 1995d). However, aging experiments with binary SiO_2/ZrO_2 and SiO_2/TiO_2 microporous nonsupported membranes, using similar conditions as described in this study, have shown that the addition of the second component did not improve the stability of the material (de Lange et al., 1993).

Stability of Supported Membranes. Results from aging experiments with supported membranes are in agreement with the results found for the nonsupported membranes. The general trend is that the permeation rates decrease as a result of aging. This can be explained by a decreased porosity, as found for the nonsupported systems.

The separation factors, however, are not necessarily decreased. As shown for membrane Al3–Si1–M and Al3–Si2–A, aging can lead to a significant improvement of the H_2/CH_4 separation factor (see Figures 7 and 8, respectively). This strongly supports our conclusion that aging leads to a pore size decrease of microporous silica. In our study of the gas transport mechanism in microporous membranes (de Lange et al., 1995b), we concluded that silica-modified membranes have smaller pore sizes than zeolite 4A (pore diameter 0.4 nm). This conclusion was based on a combination of permeation and separation experiments. Therefore, one can expect, within limits, that the increased separation factor due to ageing is caused by a slight pore-size decrease.

Since the silica top layer densifies, cracking can occur too, unfortunately. This may be the cause for the lower activation energy for hydrogen permeation as found for membrane Al1–Si1–C (Table 3). This is also very probably the reason for the difficulty in obtaining high-quality membranes by calcination at 600 °C.

Thermal aging at 200 °C for 4 months resulted in decreased permeation rates without affecting the separation properties drastically, as can be seen in Table 4. Some densification has obviously taken place, but no severe cracking resulted from this.

Comparison of the permeation results for the membranes calcined up to 600 °C, as given in Table 5, with earlier obtained results (de Lange, 1993), clearly show that the obtained membrane quality is less than for the membranes calcined at 400 °C. The mean value for the activation energy for hydrogen for membranes calcined at 400 °C, after correction for the support influence, is around 10 kJ mol^{-1}. This indicates that microcrack formation has occurred during the treatment at 600 °C, probably due to the shrinkage of the top layer. Shrinkage can be quite severe, since nonsupported membranes were dense for nitrogen after this calcination procedure (Table 1, aged sample CC). The possible occurrence of microcracks is supported by the measured permeation rates, which are relatively high.

Improvement of the stability of supported membranes by thermal dehydroxylation has not been successful, as shown by the experiments where a higher calcination temperature was used. As already mentioned, a considerable amount of surface hydroxyls, of 6 OH per square nanometer, is present at 600 °C in small micropores with diameters of 10 Å. Therefore, the material is still hydrophillic. Furthermore, calcination at 600 °C leads to considerable densification of the silica top layer, which can cause cracking.

Literature data (Brinker and Scherer, 1990; Chapter 10) shows that an effective dehydroxylation, resulting in an increased stability of SiO_2 with respect to water, may only be obtained by replacing the hydroxyls by fluorine with gas phase modification.

The importance of relative pore size on separation factors at high temperatures is shown in Table 7. It can be seen that the separation factors of binary gas

mixtures with H_2 increase with the order of molecular size of the second gas molecule (CO_2 < CH_4 < propene < isobutane). This effect can be used to explain the observation that for membrane Al1−Si2 the separation factor for methane (Figure 8) is strongly increased due to aging, while the separation factor for H_2/isobutane seems to be slightly decreased. As has been discussed before, aging of nonsupported membranes seems to result in elimination of the larger pores (at D_{eff} = 0.75 nm). The presence of these wider micropores affects hydrogen/methane separation more seriously compared to hydrogen/isobutane separation because of the smaller difference in molecular size.

Also it can be seen from Table 7 that the ratio $\alpha(H_2/CH_4)/\alpha(H_2/CO_2) \approx \alpha(CO_2/CH_4)$, which holds also for the ratio of $\alpha(H_2/\text{propene})/\alpha(H_2/CO_2) \approx \alpha(CO_2/\text{propene})$. This may indicate that the interactions of the gases with each other with the used configuration, and at these high temperatures are probably low. This is in agreement with the model of gas transport at these high temperatures as proposed earlier (de Lange, 1993, 1995b). The occupation in the micropores is for the given conditions very low, and the sorption from the gas phase follows Henry's Law.

From Table 8 it is seen that the separation factor for H_2/propene and H_2/isobutane decrease as the feed pressure is increased. This can be explained by the fact that the sorption capacity of propene and isobutane will increase stronger as function of pressure compared to hydrogen. Due to the relatively high temperature, and the only slight decrease in separation factor, the sorption process can probably still be described according to Henry's Law. Consequently, the concentration of propene and isobutane will increase stronger in the pores compared to hydrogen, leading to lower H_2/− selectivities.

If Henry's Law is not followed, due to increased concentration caused by temperature decrease and/or pressure increase, the separation factor can even decrease below 1, as has been shown by Bakker and Geus for MFI-zeolite membranes with methane/butane separation at low temperatures (Geus et al., 1992; Bakker et al., 1993). These authors report that due to strong adsorption of butane, the methane permeation is hindered. Contrary to high temperatures, where methane is permeating faster, leading to a separation factor of 0.6 for *isobutane/methane* at 350 °C, the separation factor at 27 °C is then 53 (Bakker et al., 1993) (note: isobutane permeates faster).

Since aging primarily leads to pore size decrease, accompanied by densification, it is in principle not a negative property from the viewpoint of gas separation, provided the formation of microcracks can be avoided.

However, for example in membrane reactors, it is very important to maintain a high flux (Zaspalis et al., 1992, Keizer et al., 1993). Densification is therefore not wanted. This implies that the applicability of the present type sol−gel-derived microporous silica membranes is probably limited to membrane reactors having low water partial pressure, and which are operating at temperatures lower than 350−400 °C.

Conclusions

Both thermal aging and chemical aging lead to varying degrees of densification and pore-size decrease of microporous sol−gel-derived silica.

The porosity of nonsupported SiO_2 prepared under standard conditions (400 °C for 3 h) is around 35−40%. Long-term aging at ambient conditions for 16 months (fresh, 42% porosity) or aging for 80 days at 40 °C and 60% relative humidity (fresh, 38% porosity) leads to a decreased porosity of 31%. Aging at 350 °C for 10 days in a water-containing atmosphere (1.7%) leads only to a decrease in porosity from 27% to 25%.

A gradual decrease of the mean pore size is observed after aging of nonsupported membranes. The relative contribution to the bimodal pore size distribution of the weak maximum at a pore diameter of 0.75 nm seems to decrease compared to the relative contribution at 0.5 nm.

Aging for supported membranes results in decreased permeation rates due to the densification. When no microcracks are formed, this can give improved separation properties due to pore size decrease. H_2/CH_4 separation factors between 50 and 125 have been obtained. In principle, aging is not detrimental for the separation properties, unless high permeation rates are more important than high separation factors.

The formation of membranes calcined at 600 °C proved to be difficult, which is attributed to the higher densification of the top layer, leading to microcrack formation.

Acknowledgment

Special thanks go to J. H. A. Hekkink for performing many of the permeation measurements and to G. J. M. Weierink for his help with GC analysis. Dr. J. B. Rajani and Dr. J. P. Gorcester of Shell Research, Amsterdam, are gratefully thanked for H_2/CH_4 permeation measurements on long-term aged silica membranes. Shell Research, Amsterdam, is acknowledged for general financial support.

Literature Cited

Bakker, W. J. W.; Zheng, G.; Kapteijn, F.; Makkee, M.; Moulijn, J. H.; Geus, E. R.; van Bekkum, H. Single and Multi-component Transport through Metal-Supported MFI Zeolite Membranes. In *Precision Process Technology; Perspectives for Pollution Prevention*; Weynen, M. P. C., Drinkenburg, A. A. H., Eds.; Kluwer Academic Publishers: Dordrecht, The Netherlands, 1993; pp 425−436.

Bhandarkar, M.; Shelekhin, A. B.; Dixon, A. G.; Ma, Y. H. Adsorption, permeation and diffusion of gases in microporous membranes. I. Adsorption of gases on microporous glass membranes. *J. Membr. Sci.* **1992**, *75*, 221−231.

Brinker, C. J.; Scherer, G. W. *Sol-Gel Science, The Physics and Chemistry of Sol-Gel Processing*; Academic Press: San Diego, 1990.

Brinker, C. J.; Ward, T. L.; Sehgal, R.; Raman, N. K.; Hietala, S. L.; Smith, D. M.; Hua, D.-W.; Headley, T. J. Ultramicroporous silica-based supported inorganic membranes. *J. Membr. Sci.* **1993**, *77*, 165−179.

Dubinin, M. M. The potential theory of adsorption of gases and vapors for adsorbents with energetically nonuniform surfaces. *Chem. Rev.* **1960**, *60*, 235−241.

Gavalas, G. R.; Megiris, C. E.; Nam, S. W. Deposition of H_2-permselective SiO_2 films. *Chem. Eng. Sci.* **1989**, *44*, 1829−1835.

Geus, E. R.; den, Exter, M. J.; van Bekkum, H. Synthesis and Characterization of Zeolite (MFI) Membranes on Porous Ceramic Supports. *J. Chem. Soc., Faraday Trans. 1* **1992**, *88*, 3102−3109.

Gregg, S. J.; Sing, K. S. W. *Adsorption, Surface Area and Porosity*; Academic Press: London, 1982; Chapter 1.

Horváth, G.; Kawazoe, K. Method for the calculation of effective pore size distribution in molecular sieve carbon. *J. Chem. Eng. Jpn.* **1983**, *16*, 470−475.

Iler, R. K. *The Chemistry of Silica; Solubility, Polymerization, Colloid and Surface Properties and Biochemistry*. John Wiley & Sons: New York, 1979.

Julbe, A.; Guizard, C.; Larbot, A.; Cot, L.; Giroir-Fendler, A. The sol–gel approach to prepare candidate microporous inorganic membranes for membrane reactors. *J. Membr. Sci.* **1993**, *77*, 137–153.

Keizer, K.; Zaspalis, V. T.; de Lange, R. S. A.; Harold, M. P.; Burggraaf, A. J. Membrane reactors for partial oxidation and dehydrogenation reactions. In *Membrane Processes and Separation and Purification*; Crespo, J., Bödekker, K., Eds.; Kluwer Academic Publishers: Dordrecht, The Netherlands, 1994; pp 415–429.

Kitao, S.; Kameda, H.; Asaeda, M. Gas separation by thin porous silica membrane of ultra fine pores at high temperature. *Membrane* **1990**, *15*, 222–227.

Kitao, S.; Asaeda, M. Gas separation performance of thin porous silica membranes prepared by sol–gel and CVD-methods. *Key Eng. Mater.* **1991**, *61* and *62*, 267–272.

de Lange, R. S. A. Microporous sol–gel derived ceramic membranes for gas separation; synthesis, gas transport and separation properties. Ph.D. Thesis University of Twente, Enschede, The Netherlands, 1993.

de Lange, R. S. A.; Hekkink, J. H. A.; Keizer, K.; Burggraaf, A. J. Preparation and characterization of microporous sol–gel derived membranes for gas separation applications. In *Better Ceramics through Chemistry V*; Hampden-Smith, M. J., Klemperer, W. G., Brinker, C. J., Eds.; *Mat. Res. Symp. Proc.* Materials Research Society: Pittsburgh, 1992; Vol. 271, pp 505–510.

de Lange, R. S. A.; Kumar, K-N. P.; Hekkink, J. H. A.; van de Velde, G. M. H.; Keizer, K.; Burggraaf, A. J.; Dokter, W. H.; van Garderen, H. F.; Beelen, T. P. M. Microporous SiO_2 and SiO_2/MO_x (M = Ti, Zr, Al) for ceramic membrane applications; A microstructural study of the sol stage and the consolidate state. *J. Sol-Gel Sci. Technol.* **1994**, *2*, 489–495.

de Lange, R. S. A.; Hekkink, J. H. A.; Keizer, K.; Burggraaf, A. J. Formation and characterization of supported microporous ceramic membranes prepared by sol-gel modification techniques. *J. Membr. Sci.* **1995a**, *99*, 57–75.

de Lange, R. S. A.; Keizer, K.; Burggraaf, A. J. Analysis and theory of gas transport in microporous sol-gel derived ceramic membranes. *J. Membr. Sci.* **1995b**, *104*, 81–101.

de Lange, R. S. A.; Keizer, K.; Burggraaf, A. J. Characterization of microporous membrane top layers using physisorption techniques; *J. Porous Mater.* **1995c**, *1*, 139–53.

de Lange, R. S. A.; Keizer, K.; Burggraaf, A. J. Microstructural characterization of non-supported microporous ceramic membrane top layers obtained by the sol-gel process; *J. Non-Cryst. Solids* **1995d**, in press.

Lin, Y. S.; Burggraaf, A. J. Experimental studies on pore size changes of porous ceramic membranes after modification. *J. Membr. Sci.* **1993**, *79*, 65–82.

Lippens, B. C.; de Boer, J. H. Studies on Pore Systems in Catalysts V. The *t*-Method. *J. Catal.* **1965**, *4*, 319–323.

Megiris, C. E.; Glezer, J. H. E. Synthesis of H_2-Permselective Membranes by Modified Chemical Vapor Deposition. Microstructure and Permselectivity of SiO_2/C/Vycor Membranes. *Ind. Eng. Chem. Res.* **1992**, *31*, 1293–1299.

Nam, S. W.; Gavalas, G. R. Stability of H_2-permselective SiO_2 films formed by chemical vapor deposition. In *Membrane Reactor Technology*; AIChE Symposium Series, AiChE: New York, 1989; Vol. 268, pp 68–74.

Okubo, T.; Inoue, H. Single Gas Permeation through Porous Glass Modified with Tetraethoxysilane; *AIChE J.* **1989**, *35*, 845–848.

Saito, A.; Foley, H. C. Curvature and Parametric Sensitivity in Models for Adsorption in Micropores. *AIChE J.* **1991**, *37*, 429–436.

Scholze, H. Chemical durability of glasses. *J. Non-Cryst. Solids* **1982**, *52*, 91–103.

Shelekhin, A. B.; Dixon, A. G.; Ma, Y. H. Adsorption, permeation, and diffusion of gases in microporous membranes. II. Permeation of gases in microporous glass membranes. *J. Membrane Sci.* **1992**, *75*, 232–244.

Sing, K. S. W.; Everett, D. H.; Haul, R. A. W.; Moscou, L.; Pierotti, R. A.; Rouquérol, J.; Siemieniewska, T. Reporting Physisorption Data for Gas/Solid Systems with Special Reference to the determination of Surface area and Porosity (IUPAC Recommendations 1984). *Pure Appl. Chem.* **1985**, *57*, 603–619.

Tsapatsis, M.; Kim, S.; Nam, S. W.; Gavalas, G. Synthesis of Hydrogen Permselective SiO_2, TiO_2, Al_2O_3 and B_2O_3 Membranes from the Chloride Precursors. *Ind. Eng. Chem. Res.* **1991**, *30*, 2152–2159.

Uhlhorn, R. J. R.; Huis in't Veld, M. H. B. J.; Keizer, K.; Burggraaf, A. J. Synthesis of Ceramic Membranes. Part I. Synthesis of nonsupported and supported γ-alumina membranes without defects. *J. Mater. Sci.* **1992a**, *27*, 527–537.

Uhlhorn, R. J. R.; Keizer, K.; Burggraaf, A. J. Gas transport and separation with ceramic membranes. Part II: Synthesis and separation properties of microporous membranes. *J. Membrane Sci.* **1992b**, *66*, 271–288.

van der Voort, P.; Gillis-D'Hamers, I.; Vansant, E. F. Estimation of the distribution of Surface Hydroxyl groups on Silica Gel, using Chemical Modification with Trichlorosilane. *J. Chem. Soc., Faraday Trans.* **1990**, *86*, 3751–3755.

Zaspalis, V. T.; Keizer, K.; Burggraaf, A. J.; Harold, M. P. New Concepts in Reactor Applications; Membrane Reactors. In Eurogas '92; Holmer, A., Magnussen, B. F., Steineke, F., Eds.; Proceedings of The European Applied Research Conference on Natural Gas; Trondheim, Norway, June 1–3, 1992; pp A153–A161.

Received for review January 9, 1995
Accepted June 6, 1995[⊗]

IE950038Y

[⊗] Abstract published in *Advance ACS Abstracts,* September 15, 1995.